PHYSICAL REVIEW B **73**, 104115 (2006)

Bond ionicities and hardness of $B_{13}C_2$-like structured B_yX crystals (X=C,N,O,P,As)

Xiaoju Guo, Julong He, Zhongyuan Liu, and Yongjun Tian*
State Key Laboratory of Metastable Materials Science and Technology, Yanshan University, Qinhuangdao 066004, China

Jian Sun and Hui-Tian Wang
National Laboratory of Solid State Microstructures and Department of Physics, Nanjing University, Nanjing 210093, China

(Received 31 August 2005; revised manuscript received 10 February 2006; published 28 March 2006)

Based on the fact that ionicity exists in chemical bonds between identical atoms in α-boron, investigation has been performed on the influences of X atoms on the ionicities of B-B bonds in $B_{13}C_2$-like structured B_yX (X=C, N, O, P, and As) compounds. For the four types of B-B bonds in the B_{12} icosahedra of the B_yX compounds, their overlap population P, population ionicity f_h, and Phillips ionicity f_i have been calculated. Comparing to the overlap population P_c value for the structure of the regular B_{12} icosahedron, the difference between P and P_c in the distorted B_{12} icosahedron and its origin have been discussed. Our results have shown that the charge transfer occurs between B_p and B_e atoms in the distorted B_{12} icosahedra of B_yX crystals, different from the α-boron. Electronegativity of the X atom in B_yX crystals plays an important role in the ionicities of B-B bonds in the icosahedra. Among the five investigated B_yX crystals, the largest ionicity of 0.449 has been found to exist in the B_p-B_e bond in the B_6O crystal, which is comparable to that found in AlN. By taking into account the effect of the ionicities of B-B bonds in the B_{12} icosahedra on hardness, the calculated hardness is in agreement with the experimental values for B_6O and $B_{13}C_2$. In addition, the calculations of hardness indicate that B_6N is a potential superhard material, but B_6P and B_6As are not.

DOI: 10.1103/PhysRevB.73.104115 PACS number(s): 61.50.Lt, 61.66.Bi, 62.20.Qp, 71.15.Mb

I. INTRODUCTION

As a basic concept for description of the spatially asymmetric charge distribution between two bonded atoms, the ionicity has been broadly used to interpret some essential characters in solid-state physics and chemistry. The ionicity scale, which was developed by Phillips[1] and Van Vechten[2] based on dielectric theory, leads to the successful employment of ionicity in a wide variety of studies on crystal structures and band structures,[1–3] nonlinear optical susceptibilities,[4] ultraviolet reflectance, and valence band photoemission.[5]

Generally, the ionicity is considered to exist only in the chemical bond formed by two different kinds of atoms with the occurrence of charge transfer between them. However, first-principles calculations by He *et al.*[6] have shown that in the B_{12} icosahedra of α-rhombohedral boron (α-B), there exist ionicities in B-B bonds in spite of no charge transfer between the two boron atoms. Using a new ionicity scale (population ionicity scale), they have found that the maximum ionicity in the B-B bonds can be as large as 0.359. By taking into account the ionicity of every B-B bond in the B_{12} icosahedra and its effect on hardness, they have calculated the hardness of α-B, which is in good agreement with the experimental value. Thus, the ionicity could be obtained indirectly by the measurement of the hardness.

Boron-rich solids include those allotropes formed completely by elementary boron and compounds containing boron element. With the common building element of the distorted B_{12} icosahedron, boron-rich compounds exhibit similar crystal structures. Recently, the $B_{13}C_2$-like structured boron-rich compounds B_yX (X=Be, C, N, O, Si, S, P, As, and Se) have attracted considerable interest because of their potential excellent physical and chemical properties such as great hardness, low mass density, high mechanical strength, high thermal conductivity, excellent wear resistance, and high chemical inertness.[7–11] In particular, boron carbide and boron suboxide are found to be superhard materials with hardness higher than 40 GPa.[11,12] These crystals are made up of the B_{12} icosahedra and the X-B-X with $X=C$ (see Refs. 13 and 14) or X-X chains with X=N, O, P, and As.[7,9,12] For the α-B, the ratio of c/a is 2.55. The introduction of X atom into the B_yX crystals leads to the decrease of c/a, depending on the size of the introduced atom.[7] The larger is the radius of the introduced X atom, the larger is the decrease of c/a, thus giving rise to the larger distortion of B_{12} icosahedron in B_6X, and different ionicities among B-B bonds in the B_{12} icosahedron than in the α-B. Since the physical and chemical properties of crystals are directly related to the characteristics of their chemical bonds, it is important to investigate in detail the effects of the X atoms on the ionicities of B-B bonds in the B_{12} icosahedron. In the present work, first-principles calculations have been performed to investigate the effects of X (=C, N, O, P, and As) atoms on the ionicities of B-B bonds in B_{12} icosahedron of five selected B_yX crystals. Based on the microscopic model of hardness[15] and the obtained ionicities, hardness has been calculated finally for all the five crystals. These results would offer a helpful guide to the future experimental determinations of the boron content and the structures of B_yBe, B_ySi, B_yS, and B_ySe.

II. METHODS OF CALCULATION

The first-principles calculations are performed with CASTEP code based on the density functional theory (DFT).[16] The ultrasoft Vanderbilt potentials are used and the exchange-correlation terms were considered by the Perdew-Berke-Ernzerhof form of the generalized gradient approximation. During the structural optimization, the plane-wave cutoff energy E_{cut} (see Ref. 17) is chosen to be 380 eV, and Brillouin zone sampling is performed using a $6\times6\times6$ Monkhorst-Pack grid.[18] The structural optimization is performed until the energy change of per atom is less than 5×10^{-6} eV, the forces on atoms are less than 0.01 eV/Å, and all the stress components are less than 0.02 GPa. Mulliken overlap populations were integrated by a distance cutoff of 3 Å. The spin polarized DFT and smearing electronic temperature are used in the calculations of $B_{13}C_2$.

The calculated Mulliken overlap populations of the B-B bonds in the B_{12} icosahedra were used to estimate their ionicity values via the population ionicity scale, which is defined as[6]

$$f_h = 1 - e^{-|P_c - P|/P}, \tag{1}$$

where f_h is the population ionicity, P is the overlap population of a bond, P_c is the overlap population of a bond in a pure covalent crystal with specific coordinate structure or cluster. For the selected 20 known crystals with the zinc blend structure and different overlap population P, a generalized relation of $f_h = f_i^{1.36}$ between f_h and Phillips scale f_i was obtained in Ref. 6. In the calculations of the hardness and comparison of the ionicities of B-B bonds in the B_{12} icosahedron of the five B_yX crystals to those of the chemical bonds in the known crystals, for convenience, the characterization of the ionicity in the present paper was still performed by the Phillips ionicity f_i converted by the relation with f_h.

For the chemical bonds outside the B_{12} icosahedron, their ionicities were estimated by using Eq. (22b) in Ref. 3:

$$f_i = \frac{(b\Delta Z/4.8)^2}{[1 + (b\Delta Z/4.8)^2]}, \tag{2}$$

where ΔZ is the difference of the valence electrons between the two atoms forming the bond, and b is a coefficient constant that can be estimated by

$$b = (0.089 \pm 10\%)N_c^2, \tag{3}$$

where N_c is the average coordination number of the two atoms constructing the bond.

III. IONICITIES OF THE B-B BONDS IN B_{12} ICOSAHEDRA OF B_yX CRYSTALS

The $B_{13}C_2$-like structured boron-rich compounds B_yX usually have the structures similar to the α-B. Their common structural character is that they are mainly composed of the B_{12} icosahedra network. As shown in Fig. 1(a), the α-B is constructed with the B_{12} icosahedra located at the vertexes of a rhombohedral unit cell. B_4C and $B_{13}C_2$ are the two typical rhombohedral boron carbide compounds in the boron-carbon system. As shown in Fig. 1(b), the accepted structure of $B_{13}C_2$ is built with the B_{12} icosahedra clusters linked by a C-B-C chain along the main diagonal of the rhombohedron. In fact, most studies on boron carbide have dealt with the characterization of the large homogeneity region in the rhombohedral boron carbide compound solutions over a wide range of solubility from about 9 to about 20 at. % carbon.[12,19–21] In B_4C, a boron atom located at the polar site on the B_{12} icosahedron is replaced by a carbon atom.[13,22,23] Except for that, it is very similar to $B_{13}C_2$ in structure. Hence, B_4C can be written as $(B_{11}C)+(\text{C-B-C})$. Because of the appearance of B-C bonds in the $B_{11}C$ icosahedron, $B_{13}C_2$ is chosen for present investigation. In the structure of B_6X (X=N, O, P, and As) compound, no bond is formed between the X atoms along the main diagonal of the rhombohedron as shown in Fig. 1(c).

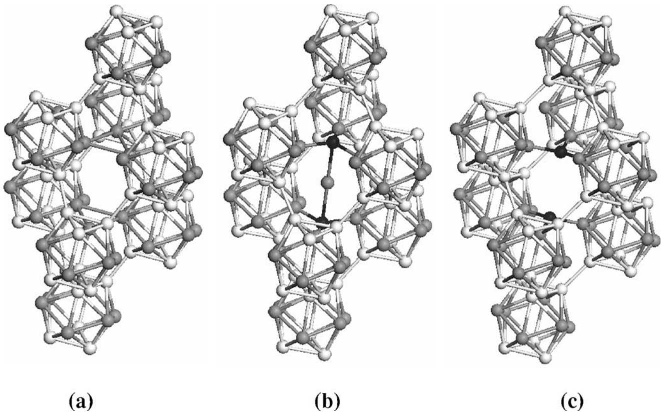

FIG. 1. Structures of α-B (a), the boron-rich compounds of $B_{13}C_2$ (b) and B_6X (X=N, O, P, and As) (c). The white spheres represent B_p atoms located at the polar sites, and the gray ones are B_e atoms at the equatorial sites in a B_{12} icosahedron. The black spheres are C or X (X=N, O, P, and As) atoms at the diagonal chain, and the gray sphere at the center of the diagonal chain is B_m atom bonded to two C atoms.

For the boron-rich B_yX compounds, there are four kinds of B-B bonds in the B_{12} icosahedra as shown in Fig. 2. The first one is the B_p-B_p bond in a B_p-B_p-B_p triangle with the three B atoms located at three polar sites. The second one is the B_e-B_e bond connecting two neighboring B atoms at the

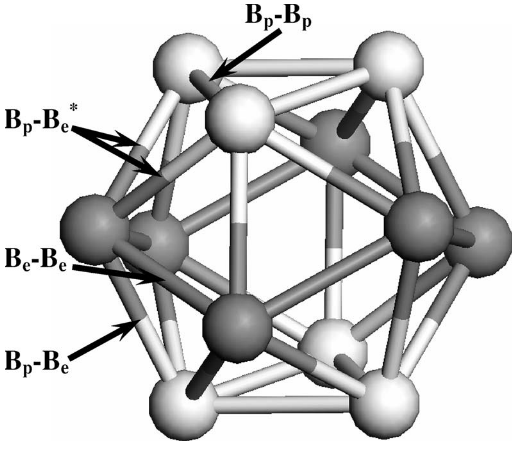

FIG. 2. The four types of B-B bonds in a B_{12} icosahedron. The white spheres represent B_p atoms located at the polar sites, and the gray ones are B_e atoms at the equatorial sites.

TABLE I. Bond lengths in B_{12} icosahedra and lattice parameters for the selected boron-rich compounds.

Crystal	B_p-B_p (Å)	B_p-B_e^* (Å)	B_p-B_e (Å)	B_e-B_e (Å)	a (Å)	α (°)
α-B	1.717	1.773	1.764	1.752	4.973	58.171
$B_{13}C_2$	1.758	1.789	1.769	1.761	5.128	65.936
B_6N	1.789	1.779	1.775	1.762	5.075	63.934
B_6O	1.758	1.757	1.786	1.732	5.080	63.264
B_6P	1.851	1.745	1.778	1.723	5.178	69.552
B_6As	1.875	1.754	1.785	1.710	5.247	70.338

equatorial sites. The rest are the two kinds of B_p-B_e bonds, which are formed between the polar and equatorial B atoms. One is denoted as the B_p-B_e^* bond, and the other is denoted as the B_p-B_e bond. Two B_p-B_e^* bonds and one B_p-B_p bond together can form a triangle B_p-B_e-B_p, while two B_p-B_e bonds cannot form a triangle with one B_p-B_p bond. In a B_{12} icosahedron, there are totally 12 B_p-B_e^* bonds, while the numbers of B_p-B_p, B_e-B_e, and B_p-B_e bonds are all equal to 6.

In Table I are listed the calculated bond lengths of the different types of B-B bonds and the lattice parameters in five boron-rich compounds. After structural relaxation, the boron-rich compounds still keep the *R-3m* symmetry. The different B-B bond lengths in each boron-rich compound indicate that the B_{12} icosahedron on each lattice site is distorted to different extents, thus losing their fivefold rotation axis. The broken geometrical symmetry in icosahedron results in the asymmetric distribution of charge density along the B-B bonds in the B_{12} icosahedra. The introduction of the X atoms breaks the three-center B_e-B_e-B_e bond in α-B, leading to the formation of three B_e-X bonds around each X atom. For the B_yX unit cells, the ratio of c/a decreases and the α angle increases with the increase of the covalent radius of the X atom. The B_p-B_p bond lengths in the boron-rich B_yX compounds are longer than those in α-B.

The overlap population P_c of the bond in the B_{12} icosahedral structure in the formula (1) has been calculated in the following way. First, a $10 \times 10 \times 10$ Å^3 cubic cell with a regular B_{12} icosahedron at its center isconstructed. After the geometry optimization, it is found that no bond is formed between two neighboring icosahedra as long as the size of the built cell is large enough. Thus, the optimized structure of the icosahedron keeps the fivefold symmetry strictly, and the calculated bond length and overlap population of B-B bonds in the icosahedron are 1.676 Å and 0.55, respectively. This overlap population of 0.55 is very close to the P_c value of 0.54 calculated from hardness.[6]

The regular B_{12} icosahedron could not be used to construct a perfect crystal because of its fivefold symmetry. In order to form the α-B or B_yX crystals with the existence of intericosahedral B-B bonds or B-X bonds, the fivefold symmetry of B_{12} icosahedra has to be removed via distortion. In the distorted B_{12} icosahedra of the α-B and B_yX crystals, the bond length of each B-B bond is longer than the B-B bond length of 1.676 Å in the regular B_{12} icosahedron, and the bond angles deviate from 60°. Comparing to the regular icosahedra, the distortions of icosahedra in α-B result in the redistribution of charge density. The elongations of intraicosahedral B-B bonds and the formations of intericosahedral B_p-B_p bonds and B_e-B_e-B_e three center bonds should result in the decrease of bond overlap population for the intraicosahedral B-B bonds in α-B. Table II lists the calculated overlap populations for the B-B bonds in the α-B and B_yX compounds. In α-B, the overlap populations of all the four types of intraicosahedral B-B bonds are lower than P_c. Among them, the B_p-B_p bonds have the lowest overlap population because of the formations of the intericosahedral B_p-B_p^* bonds with the overlap population of as high as 1.14. In the B_yX crystals, the existence of the X atoms with high charge density induces the redistribution of charge density, leading to the increase of overlap populations of some intraicosahedral B-B bonds in comparison to α-B. The overlap population can be increased so much that it is even higher than P_c of the regular B_{12} icosahedral structure. The overlap populations of the B_e-B_e bonds between the two B_e atoms bonded to the X atoms are higher than those in α-B. The overlap populations of all B_p-B_p bonds and B_e-B_e bonds in B_yX are higher than those in α-B. For the X atoms in the same row of the periodic table, such as C, N, and O, the overlap population of the B_e-B_e bond increases with the increase of electronegativity or the decrease of atomic radius of the X element. For the X atoms of N, P, and As in the same group, the overlap population of the B_p-B_p bonds increases with the decrease of electronegativity or the increase of atomic radius of the X element. In comparison to the B_p-B_p

TABLE II. Calculated Mulliken population P, population ionicity f_h and Phillips ionicity f_i of the four types of B-B bonds in B_{12} icosahedra of the selected boron-rich compounds.

	B_p-B_p			B_p-B_e^*			B_p-B_e			B_e-B_e		
Crystal	P	f_h	f_i	P	f_h	f_i	P	f_h	f_i	P	f_h	f_i
α-B	0.42	0.266	0.378	0.53	0.037	0.089	0.47	0.157	0.256	0.49	0.115	0.204
$B_{13}C_2$	0.58	0.050	0.111	0.52	0.056	0.120	0.47	0.157	0.256	0.54	0.018	0.053
B_6N	0.48	0.136	0.230	0.5	0.095	0.177	0.45	0.199	0.305	0.58	0.050	0.111
B_6O	0.52	0.056	0.120	0.55	0	0	0.39	0.337	0.449	0.64	0.131	0.225
B_6P	0.54	0.018	0.053	0.53	0.018	0.053	0.42	0.266	0.378	0:55	0	0
B_6As	0.57	0.034	0.084	0.57	0.034	0.084	0.46	0.178	0.281	0.61	0.094	0.175

TABLE III. Calculated atomic populations for the atoms located at different sites in the selected boron-rich compounds.

Atom	α-B	$B_{13}C_2$	B_6N	B_6O	B_6P	B_6As
B_p	3.0	3.04	3.03	3.07	3.02	3.13
B_e	3.0	2.88	2.79	2.75	3.16	3.26
X	—	4.64	5.53	6.55	4.46	3.84
B_m	—	2.22	—	—	—	—

and B_e-B_e bonds in the B_yX, no similar phenomena have been observed in the overlap populations of the B_p-B_e and the B_p-B_e^* bonds. It should be noted that the overlap populations of all B_p-B_e bonds in B_yX are lower than those in α-B.

Table III gives the calculated atomic populations for the atoms in α-B and B_yX. In α-B, the atomic populations for B atoms are always 3, the same as the neutral B atom, while in B_yX, the atomic populations for B atoms are quite different due to the existence of X atoms. There exists the charge transfer between the B_p and B_e atoms in the B_{12} icosahedra as well as between the B_e and the X atoms, which has never been found in the α-B. From Table III, we found that the amount of transferred charge for the B_e atom bonded with the X atom increases with the increase of the electronegativity of the X atom. When X is C, N, or O, the B_e atom would lose some charge to the X atoms. When X is P or As, the B_e atom should get some charge from the X atom. However, the B_p atom always obtains charge no matter what the X atom is. For pure covalent bonds in the regular B_{12} icosahedra, the local spatial charges on a bond distribute symmetrically. Whenever the bond population deviates from P_c, there appears the spatial asymmetric charge distribution. Figure 3 gives the typical contour maps of the charge densities along the B-B bonds. For one B-B-B triangle in a regular B_{12} icosahedron, Fig. 3(a) shows a symmetric charge distribution. For one B_p-B_e-B_e triangle in the B_{12} icosahedron of the B_6O, Figs. 3(b) and 3(c) reveal clearly the asymmetric charge distribution.

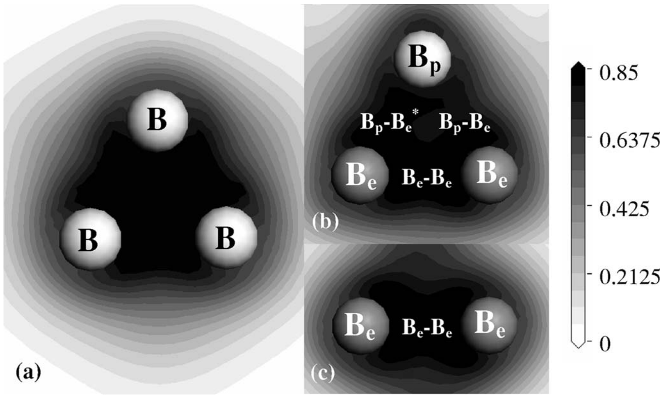

FIG. 3. Typical contour maps of the charge densities for any B-B-B triangle in a regular B_{12} icosahedron (a), the B_p-B_e-B_e triangle in the B_{12} icosahedron of the B_6O (b), and the same B_e-B_e bond as the bottom one in (b) but at a different projection plane (c).

With the overlap populations of P_c and P obtained, it is easy to calculate the population ionicity f_h and Phillips ionicity f_i using Eqs. (1). For the four types of B-B bonds in the icosahedra of the α-B and B_yX compounds, the calculated f_h and f_i are listed in Table II. In α-B, the largest ionicity is found to appear at the B_p-B_p bond in the icosahedron. The introduction of the X atom leads to obvious change in the ionicity of the B-B bond in the B_{12} icosahedron. First, the calculated ionicity of the B_p-B_p bond in the boron-rich B_yX is lower than in α-B; Second, the largest ionicity in the selected B_yX crystals appears at the B_p-B_e bond instead of the B_p-B_p bond of the icosahedron because of the effect of X atom. From Table II, in addition, we found that the electronegativity of the X atom has a great effect on the ionicities of B-B bonds if the X atom is chosen in the same row. The electronegativities of C, N, and O are 2.55, 3.04, and 3.44, respectively. The ionicity of the B_p-B_e bond increases from 0.256 in $B_{13}C_2$ to 0.449 in B_6O. In the triangle of B_p-B_e-B_e in B_6O, the B_p-B_e^* bond has no ionicity, while the B_p-B_e bond has the largest ionicity and the lowest bond population among all the B-B bonds in B_yX, and the B_e-B_e bond has a larger bond population than P_c in the regular B_{12} icosahedron. The ionicity depends on the charge distribution. The bigger the asymmetry of the charge density distribution is, the bigger the ionicity. Figures 3(b) and 3(c) give the contour map of the charge densities in the triangle B_p-B_e-B_e of B_6O, displaying distinctly the asymmetric charge distribution. For the B_p-B_e^* bond in B_6O with the overlap population of 0.55, its contour map of the charge density is the same as that of the B-B bond in the regular B_{12} icosahedron as shown in Fig. 3(b). Therefore, no ionicity exists on this bond. For the B_p-B_e bond in B_6O, the charge density around the B_e atom is much higher than that of B_p atom, resulting in the highest ionicity on the B_p-B_e bond. Obviously, the charge density of the B_e-B_e bond is higher than those of the other B-B bonds in the icosahedron. Furthermore, the charge density distributions of the icosahedra in the $B_{13}C_2$, B_6N, and B_6As tend to be uniform, leading to the decrease of the ionicity in the B-B bond of icosahedra.

IV. VICKERS HARDNESS OF THE B_yX CRYSTALS

In the B_6X (X=N, O, and As) crystals, in addition to the four kinds of B-B intraicosahedral bonds, there exists one kind of B_e-X bond around the X atom and one kind of B-B bond between the two B_p atoms in two neighboring B_{12} icosahedra. This B-B bond is denoted as B_p-B_p^*. In B_6P, surprisingly, the population of P-P bond is found to be 0.66, exhibiting that the two P atoms are bonded.[24] In $B_{13}C_2$, there is one more kind of B_m-C bond along the C-B-C chain in addition to the six kinds of bonds in B_6O. In order to calculate the hardness of the selected B_yX crystals, the Phillips ionicities for the intericosahedral bonds of B_p-B_p^*, B-C, B-N, B-O, B-P, P-P, and B-As have been calculated from Eqs. (2) and (3). The calculated Phillips ionicities and the lengths of these bonds are listed in Table IV.

According to the microscopic model of hardness for the polar covalent compounds,[15] the hardness of these four B_yX

TABLE IV. Lengths and Phillips ionicities of chemical bonds outside icosahedra in the selected boron-rich compounds.

Bond	Parameter	$B_{13}C_2$	B_6N	B_6O	B_6P	B_6As
B_e-X	d (Å)	1.590	1.464	1.484	1.888	1.965
	f_i	0.177	0.361	0.559	0.462	0.361
B_p-B_p^*	d (Å)	1.753	1.670	1.680	1.719	1.752
	f_i	0	0	0	0	0
B_m-C	d (Å)	1.420	—	—	2.215	—
or P-P	f_i	0.027	—	—	0	—

crystals should be calculated in the same way as for the multicomponent compounds. B_6N, B_6As, and B_6P have an even number of electrons in the unit cell which consists of two formulas of B_6X (X=N, O, As, and P), while $B_{13}C_2$ has an odd number of electrons. It should be noticed here that $B_{13}C_2$ has been shown to be metallic in the calculations of band structures,[25,26] but experimentally, it has been demonstrated to be semiconducting.[27] The real structure of $B_{13}C_2$ is extremely complex. For the boron carbides in ideal crystals, the electron deficiencies are often compensated by the structural defects. In the case of $B_{13}C_2$, real crystal with the valence band completely filled is energetically more favorable than the ideal structure of B_{12}(C-B-C).[27] Because the lattice parameters of ideal structure is in good agreement with the experimental data for $B_{13}C_2$,[26] it is proper to use the ideal structure of $B_{13}C_2$ to estimate the hardness instead of the real structure. As an example, a detailed description has been offered below on calculation of the Vickers hardness of B_6O. In B_6O, there are 39 bonds in total in its rhombohedral unit cell, 6 B_p-B_p, 12 B_p-B_e^*, 6 B_p-B_e and six B_e-B_e bonds in the B_{12} icosahedron, 3 B_p-B_p^* bonds between the two B_{12} icosahedra, and six B_e-O bonds. Therefore, its Vickers hardness can be expressed as

$$H_v = [(H_v^{B_p-B_p})^6(H_v^{B_p-B_e^*})^{12}(H_v^{B_p-B_e})^6 \times (H_v^{B_e-B_e})^6(H_v^{B_p-B_p^*})^3(H_v^{B_e-O})^6]^{1/39}, \qquad (4)$$

where $H_v^\mu = 350(N_e^\mu)^{2/3}e^{-1.191f_i^\mu}/(d^\mu)^{2.5}$ is the hardness of hypothetical binary compound composed of a μ bond. For each B_m-B_n bond, its valence electron density $N_e^{B_m\text{-}B_n}$ can be expressed as

$$N_e^{B_m-B_n} = [2Z_B/N_B]\left[\sum_\mu (d^\mu)^3 N^\mu\right] \Big/ [V(d^{B_m-B_n})^3], \qquad (5)$$

where Z_B is the valence electron number of the B atom, N_B is the nearest coordination number of the B atom, $d^{B_m-B_n}$ is the bond length of the B_m-B_n bond, and N^μ and d^μ are the number and length of the μ bond in one unit cell, respectively. For each B-O bond, the valence electron density $N_e^{\text{B-O}}$ can be written as

$$N_e^{\text{B-O}} = [Z_B/N_B + Z_O/N_O]\left[\sum_\mu (d^\mu)^3 N^\mu\right] \Big/ [V(d^{\text{B-O}})^3], \qquad (6)$$

where Z_O and N_O are the valence electron number and the nearest coordination number of the O atom, respectively, $d^{\text{B-O}}$ is the bond length of the B-O bond. In the structure of the B_6O crystal, the valence electron numbers of the B and O atoms are 3 and 6, respectively, while their nearest coordination numbers are 6 and 3, respectively. The other parameters used in the hardness calculation and the calculated Vickers hardness for the B_6O crystal are presented in Table V. The Vickers hardness of the B_6N, B_6P, B_6As, $B_{13}C_2$ and α-B crystals have been calculated in the same way described above, and the parameters used in the hardness calculations and the calculated Vickers hardness are listed in Table V. The calculated hardness of the B_6O and $B_{13}C_2$ is 43 and 44 GPa, respectively, in good agreement with the experimental values of 45 GPa (see Ref. 11) or 38 GPa (see Ref. 28) for B_6O and 45 GPa (see Ref. 12) for $B_{13}C_2$. For the B_6N, B_6P, and B_6As, their predicted values of the Vickers hardness are 41, 36, and 33 GPa, respectively. These results indicate that the B_6N crystal is a potential superhard material with the Vickers hardness higher than 40 GPa.

To get a deep insight into the effects of the X atoms on the Vickers hardness of the boron-rich compounds, we have calculated the hardness of icosahedra in these boron-rich compounds using the following equation

$$H_v^{\text{icosah}} = [(H_v^{B_p-B_p})^6(H_v^{B_p-B_e^*})^{12}(H_v^{B_p-B_e})^6(H_v^{B_e-B_e})^6]^{1/30}. \qquad (7)$$

The calculated results are listed in Table V. It can be seen clearly that the B_{12} icosahedron makes a dominant contribution to the hardness of the α-B. Introduction of the X atom into the diagonal chain leads to an obvious decrease of the hardness of B_{12} icosahedron in the rhombohedral cell, especially for X=N and As. For X=C, N, and O, however, the formation of shorter B_e-X or B_m-X bond can compensate for the loss of hardness of the B_{12} icosahedron, leading to the hardness of B_6O, $B_{13}C_2$, and B_6N higher than 40 GPa. Comparing the contributions of the chemical bonds outside the B_{12} icosahedron in the B_6P and B_6As on hardness to those in the α-B, we find that the hardness of the hypothetical binary compounds composed of the B_p-B_p^* bonds in the B_6P and B_6As is much lower than that in the α-B. The hardness of the hypothetical binary compounds composed of B_e-P, P-P, and B_e-As bonds is also lower than those of icosahedra in the B_6P and B_6As. Therefore, it is easy to understand that the hardness of the B_6P and B_6As crystals is lower than that of the α-B. Usually, bulk moduli are correlated to hardness, especially for the materials with the same crystal structures. The calculated bulk moduli for the five boron-rich compounds are listed in Table V. The compounds of B_6O, B_6N, B_6P, and B_6As have the same crystal structures, so their hardness increases with their bulk moduli. The bulk modulus of B_6N is almost equal to that of B_6O, supporting our prediction that B_6N is also a potential superhard material.

V. CONCLUSION

In summary, five selected boron-rich B_yX compounds have been investigated using first principles calculations to understand the influence of the X atom on the ionicities of

TABLE V. Bond parameters, calculated Vickers hardness and bulk moduli of the selected boron-rich compounds. $H_{v\,\mathrm{calc}}$ and $H_{v\,\mathrm{expt}}$ represent the calculated and experimental hardnesses, respectively.

Crystal	Bond type	N^u	d^u (Å)	N_e^μ (electron Å^{-3})	f_1^μ	H_v^μ (GPa)	H_v^{icosah} (GPa)	$H_{v\,\mathrm{calc}}$ (GPa)	$H_{v\,\mathrm{expt}}$ (GPa)	B_{cal} (GPa)
B_6O	B_p-B_p	6	1.758	0.364	0.120	37.7	36	43	45[b], 38[c]	237, 222[d]
	B_p-B_e^*	12	1.757	0.364	0	43.6				
	B_p-B_e	6	1.786	0.347	0.449	23.7				
	B_e-B_e	6	1.732	0.380	0.225	35.6				
	B_p-B_p^*	3	1.680	0.417	0	53.4				
	B_e-O	6	1.484	1.511	0.559	88.3				
$B_{13}C_{12}$	B_p-B_p	6	1.758	0.365	0.111	38.2	36	44	45[a]	227, 217[d]
	B_p-B_e^*	12	1.789	0.346	0.120	35.0				
	B_p-B_e	6	1.769	0.358	0.256	31.3				
	B_e-B_e	6	1.761	0.363	0.053	40.6				
	B_p-B_p^*	3	1.753	0.368	0	44.2				
	B_e-C	6	1.590	0.740	0.177	72.8				
	B_m-C	2	1.420	1.732	0.027	203.4				
B_6N	B_p-B_p	6	1.789	0.350	0.230	30.9	33	41	—	236
	B_p-B_e^*	12	1.779	0.357	0.177	33.7				
	B_p-B_e	6	1.775	0.358	0.305	29.3				
	B_e-B_e	6	1.762	0.366	0.111	38.1				
	B_p-B_p^*	3	1.670	0.430	0	55.3				
	B_e-N	6	1.464	1.383	0.361	109.0				
B_6P	B_p-B_p	6	1.851	0.312	0.053	32.4	37	36	—	211
	B_p-B_e^*	12	1.745	0.372	0.053	42.3				
	B_p-B_e	6	1.778	0.352	0.378	26.4				
	B_e-B_e	6	1.723	0.387	0	47.7				
	B_p-B_p^*	3	1.719	0.389	0	48.2				
	B_e-P	6	1.888	0.637	0.462	26.5				
	P-P	1	2.215	0.182	0	28.4				
B_6As	B_p-B_p	6	1.875	0.282	0.084	28.3	34	33	—	185, 182[d]
	B_p-B_e^*	12	1.754	0.344	0.084	38.2				
	B_p-B_e	6	1.785	0.326	0.281	27.9				
	B_e-B_e	6	1.710	0.371	0.175	38.4				
	B_p-B_p^*	3	1.752	0.345	0	42.4				
	B_e-As	6	1.965	0.530	0.361	27.6				
α-B	B_p-B_p	6	1.717	0.528	0.378	37.7	40	40	42[a]	217, 207[d]
	B_p-B_e^*	12	1.773	0.445	0.089	43.9				
	B_p-B_e	6	1.764	0.452	0.256	36.8				
	B_e-B_e	6	1.752	0.426	0.204	38.2				
	B_p-B_p^*	3	1.650	0.595	0	70.8				
	B_e-B_e^*	6	1.984	0.293	0	27.9				

[a] Reference 12.

[b] Reference 11.

[c] Reference 28.

[d] Reference 29.

the B-B bonds in the B_{12} icosahedra of the $B_{13}C_2$-like structured B_yX compounds. It can be concluded that the effect of the X atoms on the bond length, overlap population, population ionicity f_h and Phillips ionicity f_i of the B-B bond in B_{12} icosahedron is dependent on the electronegativity and the atomic radius of the X atoms. With the X atoms in the same row of the periodic table, the electronegativity plays a dominant role in the effect; while with the X atoms in the same group, the atomic radius plays a dominant role. Our calculations show that the ionicity of the chemical bond formed by the identical atoms such as the B-B bond could be quite different even in the same structure. The B_p-$B_e$bond in the B_6O exhibits the largest ionicity of 0.449 among all of the B-B bonds in the five B_yX crystals, which is comparable to the ionicity of AlN. There exists the occurrence of charge transfer between the B_p and B_e atoms in the distorted B_{12} icosahedra of the B_yX, while no charge transfer occurs between the B atoms in α-B. For B_6O and $B_{13}C_2$, the calculated hardness is 43 GPa and 44 GPa, respectively, in good agreement with the experimental values. Our hardness calculations predict that the B_6N crystal is a potential superhard material.

ACKNOWLEDGMENTS

This work was supported by National Natural Science Foundation of China (Grant Nos. 50225207, 10325417, 50372055, and 50472051) and by National Basic Research Program of China (Grant No. 2005CB724400).

---

*Email address: fhcl@ysu.edu.cn

[1] J. C. Phillips, Rev. Mod. Phys. **42**, 317 (1970).
[2] J. A. Van Vechten, Phys. Rev. **187**, 1007 (1969).
[3] B. F. Levine, J. Chem. Phys. **59**, 1463 (1973).
[4] S. H. Wei and A. Zunger, Phys. Rev. B **60**, 5404 (1999).
[5] J. C. Phillips and J. A. Van Vechten, Phys. Rev. B **2**, 2147 (1970).
[6] J. He, E. D. Wu, H. T. Wang, R. P. Liu, and Y. J. Tian, Phys. Rev. Lett. **94**, 015504 (2005).
[7] T. Lundström and Y. G. Andreev, Mater. Sci. Eng., A **209**, 16 (1996).
[8] F. Thevenot, J. Eur. Ceram. Soc. **6**, 205 (1990).
[9] H. Hubert, B. Devouard, L. A. J. Garvie, M. O'Keeffe, P. R. Buseck, W. T. Petuskey, and P. F. McMillan, Nature (London) **391**, 376 (1998).
[10] T. Lundström, J. Solid State Chem. **133**, 88 (1997).
[11] D. W. He, Yusheng Zhao, L. Daemen, J. Qian, T. D. Shen, and T. W. Zerda, Appl. Phys. Lett. **81**, 643 (2002).
[12] E. Amberger and W. Stumpf, in *Gmelin Handbook of Inorganic Chemistry*, edited by K.-C. Buschbeak (Springer, Berlin, 1981), pp. 112–238.
[13] F. Mauri, N. Vast, and C. J. Pickard, Phys. Rev. Lett. **87**, 085506 (2001).
[14] I. A. Howard, C. L. Beckel, and D. Emin, Phys. Rev. B **35**, 9265 (1987).
[15] F. M. Gao, J. L. He, E. D. Wu, S. M. Liu, D. L. Yu, D. C. Li, S. Y. Zhang, and Y. J. Tian, Phys. Rev. Lett. **91**, 015502 (2003).
[16] M. D. Segall, P. L. D. Lindan, M. J. Probert, C. J. Pickard, P. J. Hasnip, S. J. Clark, and M. C. Payne, J. Phys.: Condens. Matter **14**, 2717 (2002); Materials Studio, Version 2.20 (Accelrys Inc., 2003).
[17] J. P. Perdew, K. Burke, and M. Ernzerhof, Phys. Rev. Lett. **77**, 3865 (1996).
[18] H. J. Monkhorst and J. D. Pack, Phys. Rev. B **13**, 5188 (1976).
[19] M. Bouchacourt and F. Thevenot, J. Less-Common Met. **82**, 219 (1981).
[20] D. R. Tallant, T. L. Aselage, A. N. Campbell, and D. Emin, Phys. Rev. B **40**, 5649 (1989).
[21] U. Kuhlmann and H. Werheit, Solid State Commun. **83**, 849 (1992).
[22] R. Lazzari, N. Vast, J. M. Besson, S. Baroni, and A. Dal Corso, Phys. Rev. Lett. **83**, 3230 (1999).
[23] N. Vast, J. M. Besson, S. Baroni, and A. Dal Corso, Comput. Mater. Sci. **17**, 127 (2000).
[24] R. S. Mulliken, J. Chem. Phys. **23**, 1833 (1959).
[25] Dong Li and W. Y. Ching, Phys. Rev. B **52**, 17073 (1995).
[26] D. M. Bylander and Leonard Kleinman, Phys. Rev. B **43**, 1487 (1990).
[27] R. Schmechel and H. Werheit, J. Solid State Chem. **154**, 61 (2000).
[28] H. Hubert, L. A. J. Garvie, B. Devouard, P. R. Buseck, W. T. Petuskey, and P. F. McMillan, Chem. Mater. **10**, 1530 (1998).
[29] Seongbok Lee, D. M. Bylander, and Leonard Kleinman, Phys. Rev. B **45**, 3245 (1992).